



Cooling of office buildings in cold climates using direct ground-coupled active chilled beams

Downloaded from: <https://research.chalmers.se>, 2021-08-31 11:42 UTC

Citation for the original published paper (version of record):

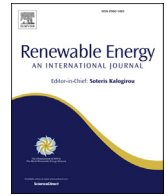
Arghand, T., Javed, S., Trüschel, A. et al (2021)

Cooling of office buildings in cold climates using direct ground-coupled active chilled beams

Renewable Energy, 164: 122-132

<http://dx.doi.org/10.1016/j.renene.2020.09.066>

N.B. When citing this work, cite the original published paper.



Cooling of office buildings in cold climates using direct ground-coupled active chilled beams



Taha Arghand^{*}, Saqib Javed, Anders Trüschel, Jan-Olof Dalenbäck

Division of Building Services Engineering, Department of Architecture and Civil Engineering, Chalmers University of Technology, 412 96, Gothenburg, Sweden

ARTICLE INFO

Article history:

Received 16 January 2020
 Received in revised form
 1 September 2020
 Accepted 14 September 2020
 Available online 17 September 2020

Keywords:

Direct ground cooling system
 High-temperature cooling
 Borehole heat exchanger
 Active chilled beam
 Design optimisation

ABSTRACT

This study investigates the use of a direct ground cooling system (DGCS) using active chilled beams for the cooling of office buildings in Sweden. The methodology of the study entails laboratory experiments to develop and validate a simulation model of the cooling system. The sensitivity of the input parameters, such as borehole heat exchanger (BHE) length, internal heat gains and room temperature set point, are studied with respect to BHE outlet fluid temperature and room thermal comfort. The results provide a practical insight into designing DGCSs with regard to borehole outlet fluid temperatures. The results also show that the thermal comfort criteria in the room are met by applying the DGCS even under the most critical design conditions of undisturbed ground temperature and internal heat gains. The sensitivity study quantifies the influence of the room temperature setpoint and internal heat gain intensity on the BHE length. The BHE outlet temperature level is more sensitive in shorter BHEs than in the longer ones, and BHE length and room temperature levels are highly correlated. Thus, the sizing of DGCS can benefit from a control system to allow the room temperature to float within a certain range.

© 2020 The Authors. Published by Elsevier Ltd. This is an open access article under the CC BY license (<http://creativecommons.org/licenses/by/4.0/>).

1. Introduction

Systems utilising ground as a heat source or heat sink are among the most viable solutions for the provision of energy-efficient space heating and cooling. For cooling purposes, ground-coupled systems benefit from exchanging heat with the ground, which has a lower temperature than the ambient air in summer. The ground temperature below a depth of seasonal temperature fluctuations (10–15 m) remains fairly constant throughout the year and only increases slowly with depth due to the geothermal gradient [1,2]. In Sweden, the underground temperature at 100-m depth varies from 3 °C in the north to 10 °C in the south [3].

The reversible ground-source heat pump system is a well-known ground-coupled cooling technology. The heat pump uses the ground as a heat sink in summer to cool the refrigerant in the condenser. Although ground-source heat pumps yield better energy performance than air-cooled chillers do [4–6], this technology also demands significant amounts of electricity for the refrigeration cycle. The typical cooling performance of such systems, defined as the ratio of the delivered thermal cooling power to the electrical

power, is between 2 and 4 [7].

In certain cases, it is also possible to use direct ground cooling systems (DGCS) to provide cooling to buildings. These systems do not use compressors and use natural ground temperatures to provide cooling [8]. DGCSs work by circulating the warm fluid from a building's terminal units down into a group of pipes inserted in vertical boreholes near the site [9]. The building's pipework can be either directly connected to the borehole or separated by means of a heat exchanger. The DGCSs use far less electricity, needed only to operate the circulation pumps. Therefore, the cooling performance ratio of the systems is as high as 13–25 [8,10].

DGCSs are often coupled with high-temperature cooling terminal units. These terminal units utilise high-temperature chilled water, usually ranging from 16 °C to just below room temperature [11], to provide space cooling. Studies on ground-coupled high-temperature cooling terminal units have evaluated the energy use of DGCSs and investigated the indoor thermal environment established by various systems, including pipe-embedded wall systems, studied by Romani et al. [12,13] and Li et al. [14]; radiant floor heating and cooling systems, by Javed et al. [15]; thermally activated building systems (TABS), by Pahud et al. [16], Eicker and Vorschulze [8] and Liu et al. [17]; ceiling cooling panels, by Arghand et al. [18]; and fan-coil units, by Li et al. [19]. In practice, the

^{*} Corresponding author.

E-mail address: arghand@chalmers.se (T. Arghand).

Ympäristötalo office building (6791 m²) in Helsinki, Finland [20], and the Entre Lindhagen office building (58,000 m²) in Stockholm, Sweden [21], are examples of buildings applying ground-coupled ACB systems for cooling.

The existing literature on DGCSs has mainly focused on evaluating the cooling performance of the system. For example, Javed et al. [15] investigated the optimal design of the borehole in relation to uncertainties in the ground design parameters. Pahud et al. [16] studied the balance ratio between the heat extracted from and supplied to the ground as an influential parameter affecting ground cooling power over the long run. Eicker and Vorschulze [8] carried out sensitivity studies on the cooling power of the ground in relation to several design parameters of the borehole and the ambient temperature.

The existing literature does not provide much information on the sizing and dimensioning of DGCS. Owing to the large time constant of the ground, short-term and rapid increase in the building cooling load affects the borehole outlet fluid temperature, which in turn, affects the heat extraction from the building. In fact, the main difficulty is the optimal sizing of the system considering the variations of the borehole outlet fluid temperature in relation to building cooling loads. Therefore, it is of crucial importance to consider and quantify the temperature ranges of the borehole outlet fluid and investigate its influence on the thermal performance of the building cooling system.

The main objective of this article is to investigate the potential of using a ground-coupled active chilled beam (ACB) system in cold climates, e.g. Swedish climate, for cooling of office buildings. This is achieved by analysing the BHE outlet temperatures with respect to the different design conditions of BHE length, room temperature setpoints and internal heat gains for a direct-ground coupled ACB cooling system. In addition, room thermal comfort is investigated with regard to the borehole system's cooling capacity with different lengths and undisturbed ground temperatures.

2. Design parameters of a DGCS

The primary concept in DGCS is to utilise the ground thermal mass potential to cool the heat transfer medium circulating between the boreholes and the building terminal units. Given the fact that the ground temperature changes under imbalanced annual heat rejection conditions, it is desirable to have a thermally balanced ground-coupled system. In such a system, the annual ground temperature remains approximately unchanged over the years of operation. This can be ensured by injecting and extracting heat to and from the ground during the summer and winter periods, respectively. The DGCS considered in this article is a thermally balanced ground-coupled system where the ground temperature increase over the years is insignificant.

The design of a DGCS requires consideration of different parameters regarding the heat transfer rates between the ground and building. Thus, sizing and design optimisation of the system is performed while taking into account the local geological properties of the ground as well as the thermal requirements of the building.

The common way for designers to size a borehole system is to specify the local ground thermal properties, the peak hourly and monthly building cooling loads and the heat loads on the BHEs for determining the appropriate arrangement of the BHEs based on these characteristics [22]. The design should guarantee the operation of the system during the entire cooling period, including the peak cooling period. Thus, both the short-term (daily and seasonal) and long-term (yearly) thermal behaviour of the ground are considered in the system design.

Designing the ground-coupled terminal units is mainly based on the outlet fluid temperatures from the borehole system. The outlet

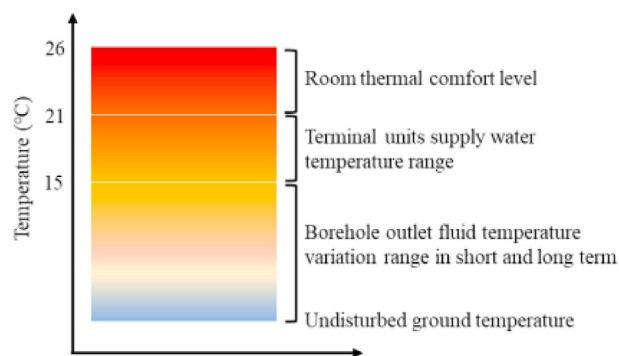


Fig. 1. Typical temperature levels in a direct ground-coupled cooling system in cold climates.

temperatures are used to design and size the building terminal units, which usually operate within a range of 16 °C to just below room temperature [23]. However, the outlet fluid temperatures undergo short-term and long-term drifts. While the short-term temperature drifts are mainly related to the building's cooling load rates, the borehole design and the ground's thermal properties, the long-term variations are associated with annual building cooling energy and the ground heat storage characteristics.

Kottek et al. [24] classified the world climate based on the monthly mean temperature of the warmest and the coldest months as well as the lowest and the highest precipitation during the winter and summer periods. According to this classification, countries with cold climate have a long and cold winter and a cool or a warm summer. Fig. 1 shows the likely temperature levels in a DGCS for cold climates. The maximum theoretical achievable cooling power from the ground is characterised by the room temperature at one end and the ground temperature at the other end. The range of room temperatures recommended for office premises is 22 °C–27 °C [25,26], which is associated with the occupants' thermal comfort. However, the ground temperature changes based on the heat flow rate between the building and the ground. The drifts in the ground temperature influence the design and the size of the room terminal units. Therefore, the proper system design is achieved by considering the variations in the fluid temperature levels so that the maximum room temperature stays within the comfort limits. In other words, overlooking the borehole outlet temperature variations in a DGCS may have the consequence of hours of overheating in the building.

In light of the above considerations, the sensitivity studies carried out in this article include investigating the influence of the parameters affecting the heat exchange rate between the building and the borehole system, such as the building temperature set point and internal heat gain intensity. Furthermore, BHE outlet fluid temperature and room thermal comfort are investigated in relation to the BHE length.

3. Overall research methodology

The main design objective for sizing the ground-coupled cooling systems is to obtain the prescribed BHE outlet temperature under design conditions. This represents the ground loads or cooling capacity of the borehole system and is also used to size the building terminal units. In this work, the outlet temperature level is assessed in relation to BHE length, internal heat gains in the building and room temperature set point. Furthermore, since the ultimate goal of using a cooling and heating system is to establish a thermally comfortable environment for the occupants, the thermal comfort levels in the room are examined in relation to the BHE length.

This study started by conducting laboratory experiments on a mock-up of an office room to investigate the borehole outlet fluid temperature ranges for a ground-coupled ACB cooling system. Although the experiments were to be conducted in a single office room, the results were still useful for analysing the typical thermal zone of a building consisting of several offices with similar cooling loads. Therefore, the simulation model, which was first developed based on the experimental results from the laboratory room, was extended to simulate a thermal zone in an office building with realistic cooling loads.

It should be reemphasised that this study was designed for a thermally balanced DGCS operating under cold climate conditions using design inputs from Sweden. The yearly average temperature of the ground with thermally balanced DGCSs remains approximately constant if the heat rejection to and extraction from the ground are equal over the year, as explained in section 2. As a result, the BHE fluid temperatures simulated for the first year are expected to be similar for other cooling periods in other years.

The range of values for the parameters investigated in this study, including the room temperature setpoint, internal gains and occupants' comfort levels, has been chosen based on the prescribed values in the national or international standards and handbooks [26–28].

4. Experimental system

This section describes the experimental set-up and methods used to perform the measurements in the test room. The results from the experimental tests are used in section 5 to develop a model of the DGCS.

4.1. System description

The DGCS test facility is located on the campus of the Chalmers University of Technology in Gothenburg, Sweden. The main parts of the DGCS include a test room with a terminal unit, a borehole, the pipework and the control components for operating the system.

The test room was a mock-up of a single-plan office. The room had 12.6 m² of floor space (4.2 m × 3.0 m) and a ceiling 2.70 m high, reduced by 0.30 m by a drop ceiling. The drop ceiling consisted of compressed fibreglass panels. The walls had a finish of 0.012 m of gypsum board attached to 0.1 m polystyrene panel walls. The test room was in a large lab hall and was therefore protected against direct sunlight and ambient temperature fluctuations.

The test room was equipped with various heat sources to simulate actual heat gains in real offices (see Fig. 2). The internal

heat gains consisted of a thermal dummy of 75 W (6 W/m²) and lighting of 110 W (8.7 W/m²). The electrical foils on the wall and floor simulated the external heat gains from solar radiation. The heat gains intensity of the foils was either 0 or 500 W (0 or 40 W/m²), depending on the experimental conditions.

The cooling load in the test room was handled by an ACB, an integrated water-based terminal unit. In a typical ACB application, the cooling load in the room is mainly handled by the cooling coil and to some extent by the cold supply air. In this study, the water to the cooling coil was supplied by the borehole system described in section 4.2. The supply air to the ACB was provided through recirculation of the room air. Therefore, the supply air temperature was approximately equal to room temperature and thus in this study air cooling did not contribute to the thermal conditioning of the room. The supply air was provided at a constant rate of 25 l/s.

The room air temperature, the supply and return water temperatures of the ACB, and the inlet and outlet temperatures of the BHE were measured using calibrated temperature sensors. The fluid temperatures were measured using screw-in type PT-100 sensors. For the ACB, the fluid temperature sensors were located on the supply and return pipes at the closest proximity to the terminal unit. The room air temperature sensor was a probe-type PT-100. The sensor was located 1.10 m above the floor at the measurement point shown in Fig. 2. The accuracy (bias) of all PT-100 thermometers was (0.1 + 0.0017 × measured value) °C. The water flow was measured with vortex-type flow meters installed in the ground and the building loop. The flow meter sensor had an accuracy of ±1.5% of the full scale (20 l/min) and a resolution of about 0.2 l/min. The sensors were calibrated before the measurements.

The cooling capacity of the ACB was controlled using the on/off flow control method. The control system for the ACB comprised of the room air temperature sensor, a control box, a two-way control valve and a circulation pump (see Fig. 3).

4.2. Ground and borehole description

Fig. 3 shows the main parts of the borehole system, including the borehole section and the corresponding pipework. The borehole comprised of a single U-tube borehole with an active depth of approximately 80 m. The U-tube in the upper clay section was enclosed in a steel pipe and the remaining part of the U-tube was enclosed in the bedrock to the bottom. The space between the U-tube and the borehole boundary was naturally filled by groundwater, which is a common practice in Sweden [29]. Fig. 3 details the ground and borehole specifications. The data summarised in Table 1 was obtained based on the on-site thermal response test

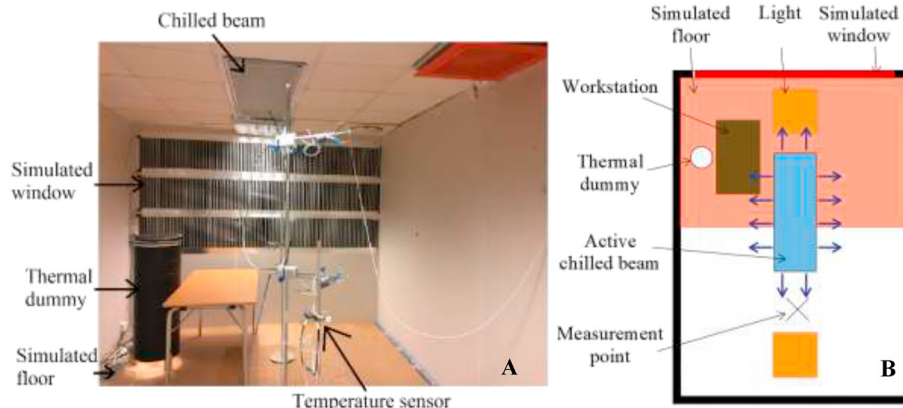


Fig. 2. A) Test-room facilities, and B) test-room layout.

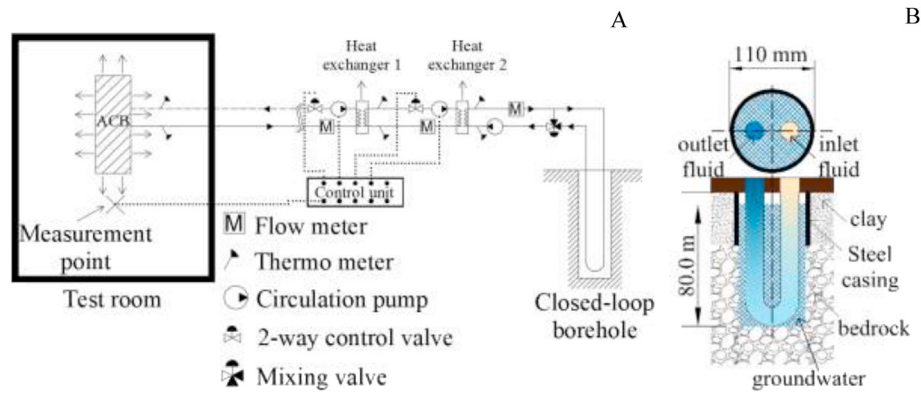


Fig. 3. A) Pipework and control components in the ground and room loops, and B) borehole cross-section.

Table 1
Ground and borehole system specifications [30].

Parameter (unit)	Specification
Borehole	
Active depth (m)	80
Diameter (mm)	110
Filling material	Groundwater
Thermal resistance (m.K/W)	0.059
Undisturbed ground temperature (°C)	8.3
Soil thermal conductivity (W/m.K)	2.88
U-tube	
Pipe type (–)	Polypropylene, PN8 DN40
Inner diameter (mm)	35.4
Outer diameter (mm)	40.0
Thermal conductivity (W/m.K)	0.42
Circulating fluid	
Type	Ethanol (29.5%)
Thermal conductivity (W/m.K)	0.401
Specific heat capacity (J/kg.K)	4180

(TRT) carried out by Javed [30]. The values for the thermal properties of the ground are typical for Sweden [3]. The borehole field has been extensively tested and reported in the literature [31,32].

The ground loop was equipped with a circulation pump and a control valve (see Fig. 3). However, the circulation rate of the heat fluid carrier in the ground loop was kept constant in this study at 0.33 ± 0.07 kg/s. The ground loop and the building loop were connected through the heat exchanger 1 (see Fig. 3).

4.3. Experimental conditions

The thermal performance of the DGCS was examined under periodic heat gain conditions in the test room. The periodic heat gains consisted of 2 h of low heat gains (16 W/m^2) and 2 h of high heat gains (55 W/m^2). The heat gain intensity was regulated by turning the electrical foils on and off. The heat gains from the lights and the thermal dummy were always constant. The duration of each heat gain period was designed based on the time constant of the room, as previously studied by Arghand et al. [33].

The experiments were performed at a room temperature set-point of $23 \text{ }^\circ\text{C}$. The control method for the ACB was on/off with no dead band. The water was circulated at a constant rate of 4.2 l/min through the terminal unit if the room air temperature was above the set point. When the room air temperature fell below the set point, the control valve was shut until the room temperature rose above the set point. A comparison between the actual room temperature and the setpoint temperature was performed by an on/off controller located in the control box.

5. Simulation model development and validation

This section describes the development and validation of a model simulating the DGCS explained in section 4. The model contained the test room and the borehole system. The model was validated against the experimental results under the experimental conditions described in section 4.3.

5.1. Simulation model

IDA ICE 4.8 simulation software was chosen to develop the model of the test room and the borehole described in section 4.2. The software is validated against measurements under the framework of various standards such as CIBSE TM33 [34], ANSI/ASHRAE 140 [35] and EN 13791 [36]. Besides, the model was validated with the data obtained from the experiments.

The borehole model in IDA ICE is based on the finite-difference approach and uses the superposition principle of heat transfer from a cylindrical 2D field around a borehole [37]. The model solves transient energy balance in the fluid, the filling material, and the surrounding ground using (1) one-dimensional heat transport equation in U-pipe liquid downward and upward with heat transfer to grout and ground, (2) one-dimensional heat equation in grout with heat transfer to liquid and ground and (3) two-dimensional heat equation in cylindrical coordinates around borehole with heat transfer to grout and liquid. It also considers the geometrical and physical properties of the ground and the surface layer, as well as the physical and thermal properties of the borehole. The model is described in detail in Ref. [38]. The simulated borehole had similar features as those shown in Table 1. However, the software considers the following assumptions in heat transfer modelling of boreholes:

- The ground is a uniform geological structure.
- The thermal resistance of the borehole is considered constant for turbulent flow.
- Vertical and horizontal seepages of groundwater are not considered.
- Vertical temperature variation in the underground is neglected.

The simulated room was modelled based on the experimental data from the test room, as described in section 4.1. The exterior side of the internal walls was exposed to the spaces with an air temperature of $20.5 \text{ }^\circ\text{C}$, equal to the exterior air temperature of the test room in the experimental set-up. A drop ceiling at 2.40 m divided the room into two spaces: the main space and the drop-ceiling space. The main space represented the area where all the internal heat sources and measurement equipment were located.

Table 2
Simulation input data for validating the DGCS for the test-room model.

Parameter (unit)	
Wall	
Thickness (m)	0.11
U-value ($\text{W}/\text{m}^2\cdot\text{K}$)	0.33
Active chilled beam	
Design cooling capacity (W)	810
Primary airflow rate (l/s)	25
Primary air temperature ($^{\circ}\text{C}$)	22.1 ± 0.3 ($T_{\text{room}} = 22.0$) 24.0 ± 0.1 ($T_{\text{room}} = 24.0$) 25.9 ± 0.2 ($T_{\text{room}} = 26.0$)
Supply water flow rate (l/min)	4.2
Supply water temperature ($^{\circ}\text{C}$)	Variable between 15.7 and 16.5
Cooling capacity control method	On/off water flow rate

The ACB was placed on the drop ceiling. Thus, only the main space was thermally conditioned by the ACB. The specifications of the simulated room are listed in Table 2.

The ACB model included an idealised supply air diffuser for the airside and a water heat exchanger to simulate the heat transfer between the air and the liquid. The supply airflow rate of the ACB was always constant at 25 l/s, with a similar temperature as the room air temperature. The supply water flow rate was constant at 4.2 l/min. The supply water temperature was variable, depending on the liquid temperature in the BHE loop and the operating period of the system. The input parameters of the ACB model are also summarised in Table 2.

5.2. Validation of the test-room model

Fig. 4 shows a comparison of the simulated and measured room air temperatures under periodic internal heat gains. The simulated results and measured data match closely, showing a small discrepancy of only ± 0.2 K. The simulated room temperature features more fluctuations. In practice, the thermal mass of the room components, such as the walls, floor and ceiling, as well as the cooling water in the coil, reduced the room temperature fluctuations to some extent. However, the model did not consider the thermal mass of the cooling water in the ACB and overlooked, to a lesser extent, the thermal mass of the furniture.

BHE outlet temperature and supply water temperature to the ACB are two important design parameters defining the ground load ranges and the cooling capacity of the terminal unit, respectively. The results in Fig. 5 show a good agreement between the simulated and measured BHE water temperatures. The experimental outlet temperature seems quite stable, suggesting that the variations in the inlet temperature did not affect the outlet temperature.

The experimental ACB supply water temperature shown in Fig. 5 has peaks and troughs because of the on/off control of the flow rate. When the control valve was shut, the standstill water in the ACB absorbed heat from the room. The water was later replaced with cold water when the control valve opened. This effect cannot be seen in the simulation because the software did not consider heat transfer between the standstill water and the surrounding. However, this issue would not make any significant difference to the energy calculation since the simulated water temperature approximately follows the average water temperature of the experiments.

5.3. Extended simulation model

The model described thus far only simulated the DGCS in the laboratory. Developing such a model was necessary to simulate the transient performance of the ground-coupled cooling system, as

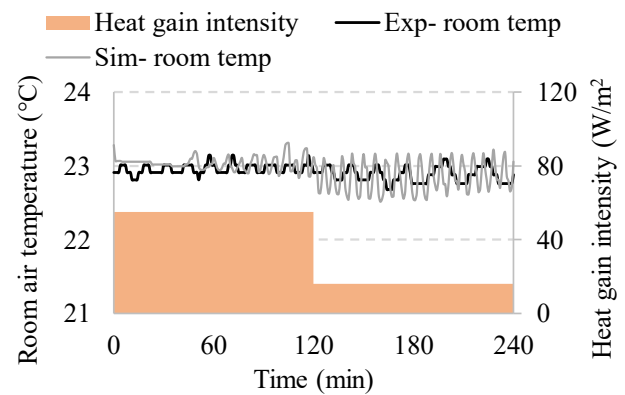


Fig. 4. Measurement data (Exp) and simulation results (Sim) on the room air temperature (temp).

well as the test room. However, due to the inherent limitations of the experimental set-up, such as the dimension of the test room, heat gain intensity and duration and BHE length, an extended model representing a more realistic office building was needed to test the operational performance of the cooling system. This section describes the extended model of the test room, which was later used for the sensitivity studies.

The extended model was developed based on the laboratory test-room model but on a larger scale (see Fig. 6). In addition, in order to simulate the external heat gain from solar radiation, the southern wall in the extended model was of the external type with a 57% window-to-wall ratio and no exterior/interior shading. The other walls were simulated as internal walls, exchanging heat with internal spaces with a constant temperature of 20.5°C , equal to the test-room model. In this way, the simulated office was approximated as a single-perimeter zone in a larger office. Internal heat gains included gains from occupants ($6 \text{ W}/\text{m}^2$), lighting ($8.7 \text{ W}/\text{m}^2$) and equipment (0 or 7.9 or $16.5 \text{ W}/\text{m}^2$). The specifications of the model envelope are listed in Table 3. The simulated office was located in Gothenburg, Sweden, and the simulation period was from May 14, 2018, to September 21, 2018.

With regard to the terminal units, the extended model included 7 ACBs for space cooling. The ACBs had a similar cooling capacity, control method and operational characteristics as those of the test-room model (see Table 3).

The undisturbed ground temperatures used in this study were 3°C and 11°C , based on the ground temperature limits at a depth of 100 m in Sweden, as provided by Rosen et al. [3]. The other parameters regarding the local geological properties of the ground and the borehole thermal specifications were the same as in the test-room model (see Table 3).

6. Sensitivity analysis results and discussion

This section contains the sensitivity studies of the extended model described in section 5.3. As previously mentioned in section 2, appropriate design of a DGCS requires consideration of the sensitivity of the temperature levels of the cooling medium in the BHE and the building cooling system. Choosing too tight a temperature range may hinder the operating of the system or result in many hours of overheating in the room. Too large a temperature range, on the other hand, would incur unnecessary expenses. The following are the results from the sensitivity study of the BHE outlet temperature and room thermal environment regarding the variations in BHE length, internal gains and room temperature setpoints.

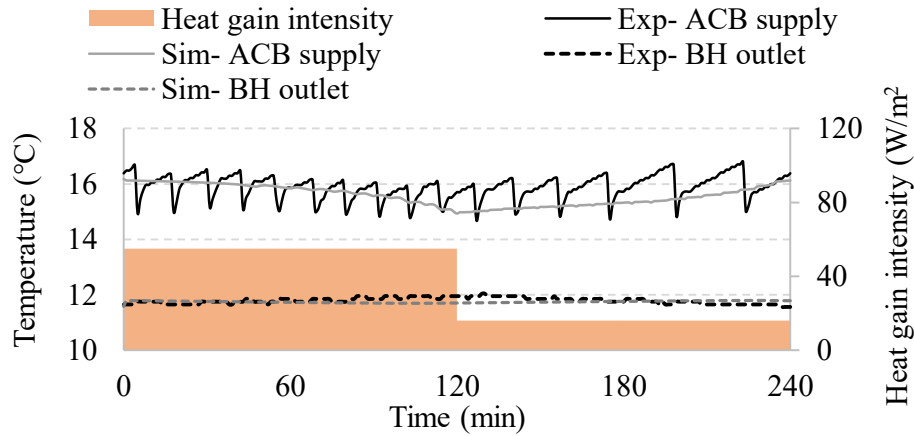


Fig. 5. Measurement data (Exp) and simulation results (Sim) for the borehole (BH) outlet and ACB supply temperatures.

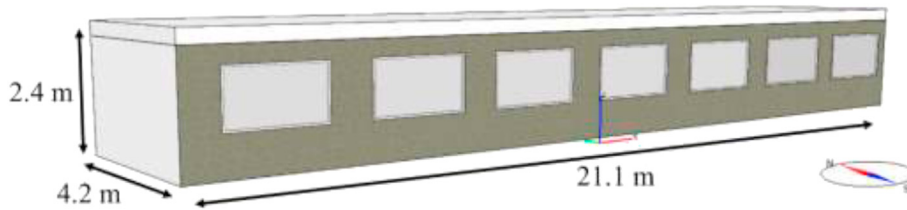


Fig. 6. Plan view of the extended test-room model representing a single-perimeter zone of an office building.

Table 3
Description of the input parameters to the extended simulation model.

Parameter (unit)	
External wall	
Dimensions (m)	21.1 × 2.4 (W × H)
U-value (W/m ² .K)	0.33
Thickness (m)	0.27
Internal wall	
Dimensions (m)	21.1 × 2.4, 4.2 × 2.4 (W × H)
U-value (W/m ² .K)	0.54
Thickness (m)	0.11
Window	
Number of windows	7
Dimensions (m)	1.2 × 2.2 (H × W)
U-value (W/m ² .K)	1.19
G-value (%)	43
Floor area (m ²)	88.7
Borehole	
Length (m)	60 - 200 (Variable based on the case study)
Undisturbed ground temperature (°C)	3 or 11 (Variable based on the case study)
BHE fluid mass flow rate (kg/s)	0.8
Other specifications	See Table 1
Active chilled beam	
Number of the ACB	7
Supply water temperature (°C)	15 - 22 (Variable based on the case study)
Other specifications	See Table 2

6.1. Influence of BHE length on borehole outlet temperature

The common approach to sizing BHEs is to adjust the borehole field size iteratively to meet the user-prescribed limits for the BHE outlet temperature. The BHE outlet temperature is usually defined to meet the peak building cooling/heating loads. Thus, BHE size is usually described in relation to the building peak loads. However, the primary aim of having any heating and cooling systems in a building is to satisfy the occupants' thermal comfort. Thus, it is

more practical, especially for DGCSs, to associate the thermal environment in the room with BHE size.

However, the aim of this section is not to evaluate the sizing methods for the BHEs, but rather to investigate the correlation between BHE size, the borehole outlet fluid temperature and the ground loads. This is done by investigating the BHE outlet temperature and ground loads, as well as the operative temperature range in the room in relation to various combinations of BHE length and climate (undisturbed ground temperature). The simulations

were performed during a cooling period from mid-May until September 20, 2018. The maximum internal heat gains were 2.8 kW (31.2 W/m²). The room temperature setpoint was 24 °C and the fluid flow rate in the BHE was constant at 0.8 kg/s and similar for all cases.

The box plots in Fig. 7 show the BHE outlet temperature spread during the cooling period for the BHE lengths. The minimum temperatures, shown by the lower whisker, are obtained at the system start-up after the weekends. The maximum values, denoted by the upper whisker, are associated with the warm days during which the peak cooling load appears. The line in the box area shows the median value of the temperature range.

Comparing the outlet temperature level, between the upper and the lower whiskers, for each BHE length, indicates that the outlet temperature level is more sensitive for the shorter BHE than for the longer ones. For instance, the outlet temperature spread for a 60 m long BHE with an undisturbed ground temperature of 3.0 °C falls between 5.0 °C and 13.9 °C, while this range is 4.0 °C–9.2 °C for a BHE of 120 m length (see Fig. 7A). This significant variation in the outlet temperature is especially important for sizing the terminal units as well as calculating the available cooling coil power. The temperature levels for the warmer ground temperature of 11.0 °C in Fig. 7B are smaller because of the higher undisturbed ground temperature.

As can be seen in the figure, the outlet temperatures are inversely proportional to the BHE length because of the increase in the heat exchange area between the fluid in the U-tube and the ground. The trend appears to be non-linear. This is partly because the difference between the mean fluid temperature and the ground temperature decreases with the BHE length, which in turn, affects the heat transfer between the fluid and the ground. Besides, heat short-circuiting between the U-tube's legs increases with BHE length, which causes an increase in the outlet temperature.

While Fig. 7 shows the temperature levels in the BHE, it is practical from the design point of view to know the achievable ground load ranges for the borehole system. Fig. 8 shows the minimum and maximum ground loads per unit length for the considered cooling demand for the simulated office. The ground loads are calculated based on the difference between the inlet and outlet fluid temperatures of the BHE. The maximum values are attributed to the peak cooling load period, while the minimum values are obtained during the start-up of the system.

The results show that the ground loads per BHE unit length are inversely proportional to BHE length. The non-linear trend is partly associated with the non-linear heat exchange rate in the BHE and is partly related to the thermal short-circuiting between the U-tube's legs. Generally, a longer BHE provides greater ground loads. However, Fig. 8 suggests considering the trade-off between the BHE

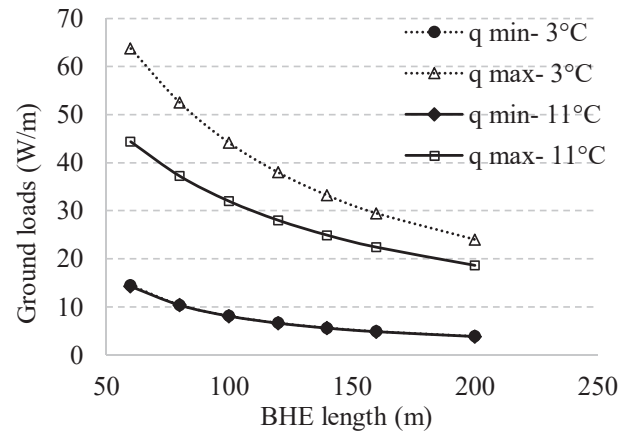


Fig. 8. Minimum (q_{min}) and maximum (q_{max}) ground load ranges in relation to BHE length and undisturbed ground temperatures. The room set point was 24 °C and the internal gains were set at 31.2 W/m².

length and the ground load ranges required for the building. It is worth noting that the minimum ground load ranges with two undisturbed ground temperatures are similar and thus they are shown with one line in Fig. 8.

6.2. Influence of room temperature set points on borehole outlet temperature

In general, the room temperature setpoint greatly affects the design of the borehole system by defining the amount of heat transferred to the ground. In fact, the setpoint influences the intensity of the peak building cooling load, which, in turn, influences the ground temperature variations in the short and long terms. This section investigates the short-term effect of the room temperature set points on the BHE outlet temperature level. The BHE outlet temperature is chosen as the output parameter because it reflects the changes in the ground loads and because it is the main parameter for sizing building terminal units.

Fig. 9 shows the box plots of the BHE outlet temperatures corresponding to the room temperature set points of 22 °C, 24 °C and 26 °C. The simulations were carried out for the entire cooling period and the internal gain was 31.2 W/m² for all cases. The results in Fig. 9 can be interpreted in two ways. The influence of the room setpoint can be seen not only in changing the BHE maximum temperature, shown by the upper whisker but also in changing the median and lowest temperatures. While changes in the maximum BHE temperature are proportionally related to the size of the terminal units, changes in the whole temperature range influence the

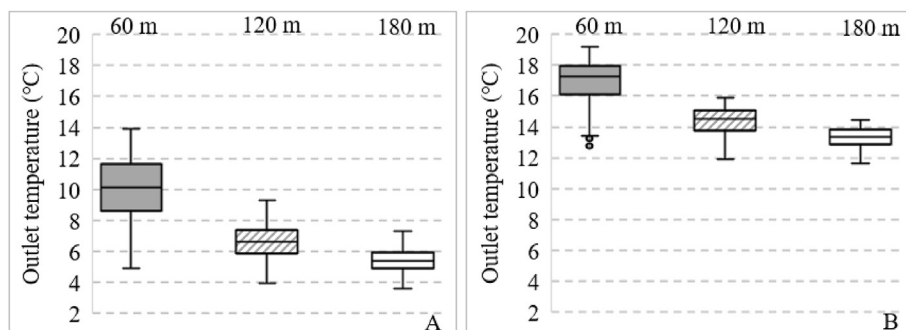


Fig. 7. BHE outlet temperatures for different lengths at undisturbed ground temperatures of A) 3 °C and B) 11 °C. The room set point was 24 °C and the internal gain was set at 31.2 W/m².

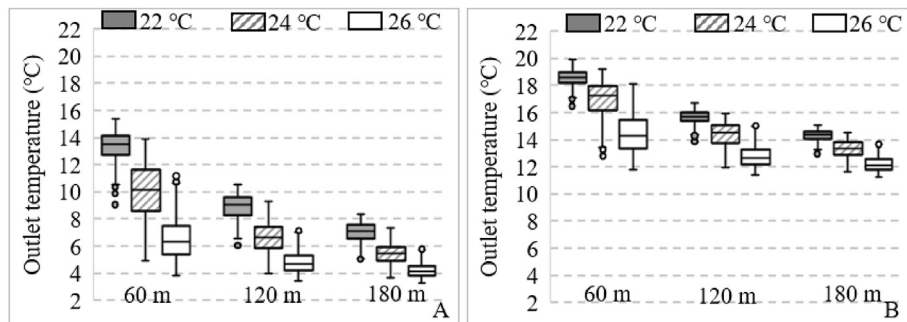


Fig. 9. BHE outlet temperature levels as a function of room temperature set point. The simulations were performed for the whole cooling period for the undisturbed ground temperature of A) 3 °C and B) 11 °C. The internal gain was 31.2 W/m² for all cases.

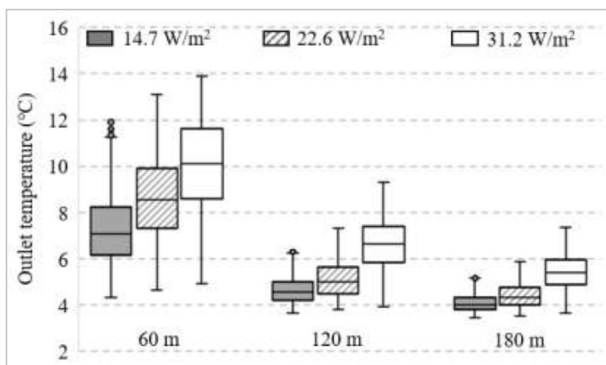


Fig. 10. BHE outlet temperature variations with internal gains simulated for BHEs of 60 m, 120 m, and 180 m. The undisturbed ground temperature was 3 °C and the room temperature setpoint was 24 °C.

water flow rate and the pump energy use in the building cooling system. This is because when the overall temperature levels of the cooling fluid medium increase, a higher flow rate is required to remove a given cooling load from the building. A change in the overall outlet temperature level with room temperature seems to be stronger for lower undisturbed ground temperatures, due to the larger difference between the fluid and the ground temperatures.

6.3. Influence of internal heat gain intensity on borehole outlet temperature

The box plots in Fig. 10 show the BHE outlet temperature levels, including the maximum, minimum and median temperatures for common internal gains in office buildings based on ASHRAE Fundamentals 2017 Chapter 18 [28]. The simulated internal loads range from 14.7 W/m², for an office with no office electrical equipment, to 31.2 W/m², for an office equipped with a workstation connected to three screens for each person and one printer for eight people. As expected, increasing the internal gain intensity causes the maximum outlet temperature to increase. It seems that the outlet temperature in the shorter BHE is more sensitive to changes in heat gains than that in the longer one. This deals with the higher available cooling capacity in the longer BHEs.

A comparison of Figs. 9 and 10 reveals that the magnitude of the changes made by changing the room set points is considerably greater than that achieved by varying the heat gains. One likely reason is that amount of the heat load changed by varying the setpoint is higher than that of the amount of heat load changed by altering the heat gains. Another explanation is the intermittent operation of the cooling system. On weekdays, the building cooling

system operates from 6:00 to 18:00, and it is off during the weekends. This intermittent operation allows the ground to recover its temperature, to some extent, during the off period, as noted elsewhere [39,40]. The influence of the operation of the system can be justified by investigating the minimum BHE outlet temperatures. The minimum outlet temperatures in Fig. 10 remained approximately unchanged when changing the internal gains. When the set points were changed, however, a considerable change could be seen in the minimum outlet temperatures (see Fig. 9). Further simulations reveal that the continuous operation of the system caused the minimum BHE outlet temperature to increase within the range of 1.5 K–4.4 K for the BHE lengths investigated in this study.

6.4. Influence of BHE length on the indoor thermal environment

The results presented so far are helpful in sizing the BHEs but it would be better still to be able to determine the room comfort criteria for different borehole design conditions. For this reason, the room's operative temperature (T_{op}) was used to evaluate the room's thermal environment, as suggested in other studies [25,26]. Simulations in this section were performed for the whole summer period. The room temperature setpoint was 24 °C. The simulated internal loads ranged from 14.7 W/m², for an office with no office electrical equipment, to 31.2 W/m², for an office equipped with a workstation connected to three screens for each person and one printer for eight people [28].

Fig. 11 presents the distribution of T_{op} during the working hours, from 6:00 to 18:00, in the cooling period. Each boxplot shows the maximum and minimum T_{op} in the room by the upper and the lower whiskers, respectively. The quartile range, that is, the area shown by the box, presents the lower quartile, median and upper quartile values. The median illustrates the middle value of all room temperatures during the simulation period. The points above the upper whisker, if any, are outliers. Temperatures lower than 24 °C are temperature undershoots caused by the time lag of the system.

Fig. 11 has three major features of interest: the T_{op} spread during the cooling period, the peak temperatures and the room thermal comfort categories. A comparison of the temperature spread enclosed between the upper and the lower whiskers show that increasing the BHE length causes a reduction in the T_{op} range. The reduction is relatively small, especially for the undisturbed ground temperature of 3 °C. This is because the temperature spread shown by each boxplot is mostly formed and influenced by the temperatures occurring during the part-load periods. Since the ground loads with a 60 m BHE is most likely enough to cool the room during the majority of the part-load periods, increasing the length does not lower the T_{op} range to any great extent.

However, increasing the BHE length is more pronounced in

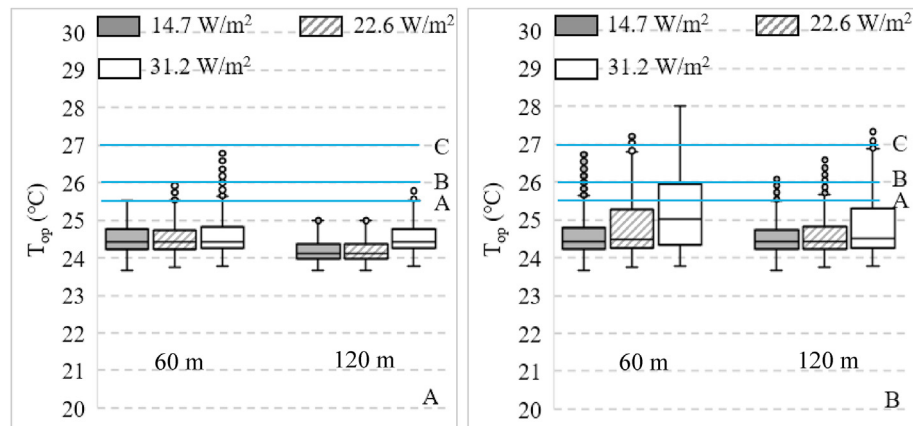


Fig. 11. Room operative temperature (T_{op}) levels simulated under different internal gains for BHE lengths of 60 m and 120 m at an undisturbed ground temperature of A) 3 °C and B) 11 °C. The blue lines represent the maximum allowed T_{op} in the room. The maximum T_{op} for categories A, B and C are 25.5 °C, 26 °C and 27 °C, respectively, based on ISO 7730 [26]. The room temperature set point is 24 °C. (For interpretation of the references to colour in this figure legend, the reader is referred to the Web version of this article.)

reducing the maximum T_{op} . Maximum temperatures occurred during the peak hour loads and are shown by the upper whisker and the outliers. As can be seen in Fig. 11 the maximum temperatures were reduced by increasing the length, since the longer BHE provides a higher cooling capacity. In fact, the influence of changing the length can best be observed in the number of overheating hours in the room. The optimum size for the BHE can be calculated by compromising between the number and/or duration of the overheating hours and the length of the ground heat exchanger.

Fig. 11 also shows the correlation between BHE length and the room thermal comfort categories. The blue lines in Fig. 11 define the maximum allowed T_{op} in the room according to the indoor thermal environment categories suggested in ISO 7730 [26]. As can be seen in the figure, categories B and C can be met with 120 m BHEs for the entire range of undisturbed ground temperatures between 3 °C and 11 °C. With the 60 m BHE, fulfilling category B and C is feasible with BHEs at a 3 °C undisturbed temperature. This result points to the idea that a ground-coupled ACB can provide a comfortable environment for the occupants even in those spaces with high cooling demand.

Although Fig. 11 shows the distribution of T_{op} during the cooling season, details regarding the number of overheating hours for different design configurations are not provided. Overheating hours occur during the peaks and their duration is proportional to the maximum cooling capacity provided by the borehole.

Table 4 summarises the number of overheating hours of T_{op} for each thermal environment category according to ISO 7730 [26]. For 95 working days during the simulated period, there were 1140 cooling hours. As can be seen in the table, both the internal gains and the BHE length affect the number of overheating hours. These factors appear to be more significant in the shorter BHE. In the longer BHE, concerns about overheating are alleviated. In general, Table 4 shows that achieving category C with the ground-coupled ACB system is viable even with short BHEs and high internal gains up to 31.2 W/m².

As can be seen from Table 4 and Fig. 11, sizing the BHE to meet the cooling peaks may result in a large BHE system. Therefore, considering some overheating hours in the design significantly contributes to reducing the cooling demand and lowering the BHE size. The extent to which the impact of overheating hours needs to be considered depends on the designed comfort levels in the room. For instance, the Swiss technical standard SIA Norm 382/1 allows a maximum room temperature of 26.5 °C for no longer than 100 h [16].

6.5. General discussion and practical implications

BHEs are usually sized to reach the user-defined BHE outlet fluid temperature. This temperature is defined based on the cooling demand of the building under peak cooling conditions. Sizing the BHEs in DGCSs based on the peak loads guarantees that the borehole system provides the necessary cooling power for the peak conditions. A detailed description of these methods can be found in other studies [41,42]. This article does not deal with sizing the BHEs but the results in section 6 can be useful for optimising their size. The results suggest designing the building temperature control system so that the room temperature increases to a certain extent during the peak period in order to reduce the peak cooling load. This peak shaving method certainly reduces the BHE length without violating the thermal comfort limits of the occupants. One example of such a design is the application of a supply temperature control method, also known as a self-regulating control method, for high-temperature cooling terminal units. In this method, the water to the terminal units is supplied at a constant flow rate and temperature. The room temperature varies within a certain range corresponding to the changes in the internal room gains. Other works have described the application of this method for ACB [43,44] and ceiling cooling panels [18]. Future work should concentrate on the challenges of sizing BHEs for different cooling capacity control methods for building terminal units.

The development of ground-coupled ACBs is attracting more attention in Scandinavian countries because ACBs are the most common high-temperature terminal units. A high cooling capacity, easy cooling capacity control and fast response for stabilising the room temperature are some of the advantages of ACBs. The Ympäristöotalo office building in Helsinki, Finland [20], and the Entre Lindhagen office building in Stockholm, Sweden [21] are examples of buildings applying ground-coupled ACB system for cooling. More studies on the long-term cooling performance of this system and how to implement it not only for cooling but also for heating purposes, especially from the ground thermal storage perspective, will encourage the widespread use of this system.

6.6. Limitations

As mentioned in section 5.1, the heat transfer modelling of boreholes in IDA ICE has certain limitations. However, these limitations can be addressed by using in-situ measured values of ground thermal properties as done in this study. The in-situ

Table 4

Number of overheating hours based on the thermal environment categories in ISO 7730 [26] for BHEs of 60 m and 120 m and various internal gains. The simulations were performed for 1140 working hours during the cooling period. The room temperature setpoint was 24 °C and the internal gains were 31.2 W/m² for all conditions. The maximum T_{op} for categories A, B and C were 25.5 °C, 26 °C and 27 °C, respectively.

	Undisturbed ground temperature (°C)	Internal heat gains (W/m ²)	Thermal comfort category A		Thermal comfort category B		Thermal comfort category C	
			60 m	120 m	60 m	120 m	60 m	120 m
3		14.7	1	0	0	0	0	0
		22.6	18	0	2	0	0	0
		31.2	72	10	28	0	0	0
11		14.7	62	22	25	3	0	0
		22.6	196	70	88	27	8	0
		31.2	400	209	262	93	46	7

measured undisturbed ground temperature accounts for the temperature gradient in the ground. Moreover, using average ground temperature instead of actual ground temperature with geothermal gradient gives trivial errors in the heat extraction performance of BHEs [45]. Similarly, the in-situ measured values of ground thermal conductivity and borehole thermal resistance account both for the non-uniform geological structure of the underground and the groundwater movement. The authors, however, recommend taking geothermal gradient and groundwater movement into account for systems with a high geothermal gradient or a significant groundwater movement and/or a small temperature difference between the undisturbed ground and the room indoor temperature. Under these circumstances, the calculated borehole outlet temperatures may deviate from the actual values.

7. Conclusions

The application of the ground-coupled ACB system for comfort cooling in an office building has been presented using experimental results at the laboratory scale and simulation results for a single-perimeter zone in a large office. Besides, sensitivity studies were performed on the parameters having an influential role in the heat exchange rate between the borehole and building, such as BHE length, room temperature setpoint and internal heat gain intensity. The sensitivity study aimed to investigate the variations of the BHE outlet fluid temperature in relation to the parameters studied. Given the experimental set-up and the simulation assumptions, the concluding remarks of this study are summarised below:

- Ground-coupled ACBs offer a viable alternative for cooling office premises in cold climates such as Sweden's. The results from the simulation models show that meeting the thermal comfort criteria recommended in ISO 7730 [26] is possible, even for the most critical design conditions, namely, an undisturbed ground temperature of 11 °C and internal gains as high as 31 W/m².
- BHE outlet temperature level is more sensitive in shorter BHEs than in longer ones. The influence of BHE length is greater on maximum BHE temperature than on median temperature. As a result, the room temperatures during the peak cooling conditions, i.e. the maximum room temperature, experience a larger change than the room temperatures during the part-load conditions through a change in the BHE length.
- The room temperature setpoint plays an important role in establishing the BHE outlet fluid temperatures because it defines the heat transfer rate to the ground. For BHEs of 60 m and 120 m, changing the room temperature setpoint from 24 °C to 26 °C caused 5.0 K and 2.7 K reduction in the maximum BHE outlet temperature, respectively. Within the same context, changing the internal gains from 14.7 W/m² (no electrical office equipment included) to 31.2 W/m² (a desktop with three

screens and one printer for eight office workers) had a modest effect on reducing the maximum BHE temperature by 2.5 K and 2.0 K for 60 m and 120 m BHEs, respectively.

- Given the results from the parametric study, we suggest designing the control system to allow the room temperature to float within a certain range. Increasing the room temperature during the peak cooling period reduces the peak intensity and requires shorter BHEs.

A likely future study will investigate the sizing of BHEs with regard to different methods for controlling the cooling capacity of direct ground-coupled ACB systems.

CRedit authorship contribution statement

Taha Arghand: Methodology, Validation, Writing - original draft, Investigation. **Saqib Javed:** Supervision, Writing - review & editing. **Anders Trüschel:** Supervision, Writing - review & editing. **Jan-Olof Dalenbäck:** Project administration, Supervision, Writing - review & editing.

Declaration of competing interest

The authors declare that they have no known competing financial interests or personal relationships that could have appeared to influence the work reported in this paper.

Acknowledgements

This work was financially supported by the Swedish Energy Agency (Energimyndigheten) through its E2B2 national research programme. The in-kind contribution of laboratory facilities by Swegon and Lindab is gratefully appreciated. We are particularly grateful to Håkan Larsson for his lab assistance. Valuable discussions with Carl-Ola Danielsson (Swegon) and Göran Hultmark (Lindab) are also acknowledged.

References

- [1] G. Florides, S. Kalogirou, Ground heat exchangers—a review of systems, models and applications, *Renew. Energy* 32 (2007) 2461–2478, <https://doi.org/10.1016/j.renene.2006.12.014>.
- [2] A. Vieira, M. Alberdi-Pagola, P. Christodoulides, S. Javed, F. Loveridge, F. Nguyen, F. Cecinato, J. Maranhã, G. Florides, I. Prodan, G. Van Lysebetten, E. Ramalho, D. Salciarini, A. Georgiev, S. Rosin-Paumier, R. Popov, S. Lenart, S.E. Poulsen, G. Radioti, Characterisation of ground thermal and thermo-mechanical behaviour for shallow geothermal energy applications, *Energies* 10 (2017), <https://doi.org/10.3390/en10122044>.
- [3] B. Rosén, A. Gabriellsson, J. Fallsvik, G. Hellström, G. Nilsson, System för värme och kyla ur mark: en nulägesbeskrivning, Swedish Geotechnical Institute (SGI), Linköping, Sweden, 2001.
- [4] H. Yang, P. Cui, Z. Fang, Vertical-borehole ground-coupled heat pumps: a review of models and systems, *Appl. Energy* 87 (2010) 16–27, <https://doi.org/10.1016/j.apenergy.2009.04.038>.

- [5] Z. Zhou, Z. Zhang, G. Chen, J. Zuo, P. Xu, C. Meng, Z. Yu, Feasibility of ground coupled heat pumps in office buildings: a China study, *Appl. Energy* 162 (2016) 266–277, <https://doi.org/10.1016/j.apenergy.2015.10.055>.
- [6] K.J. Chua, S.K. Chou, W.M. Yang, Advances in heat pump systems: a review, *Appl. Energy* 87 (2010) 3611–3624, <https://doi.org/10.1016/j.apenergy.2010.06.014>.
- [7] A. Chiasson, J.D. Spitler, Modeling approach to design of a ground-source heat pump bridge deck heating system, *Transport. Res. Rec.* 1741 (2001) 207–215.
- [8] U. Eicker, C. Vorschulze, Potential of geothermal heat exchangers for office building climatization, *Renew. Energy* 34 (2009) 1126–1133, <https://doi.org/10.1016/j.renene.2008.06.019>.
- [9] D. Banks, *An Introduction to Thermogeology: Ground Source Heating and Cooling*, John Wiley & Sons, 2012.
- [10] Y. Man, H. Yang, Y. Qu, Z. Fang, Feasibility investigation of the low energy consumption cooling mode with ground heat exchanger and terminal radiator, *Procedia Eng* 121 (2015) 423–429, <https://doi.org/10.1016/j.proeng.2015.08.1088>.
- [11] T. Arghand, Direct-Ground Cooling Systems for Office Buildings: Design and Control Considerations, Chalmers University of Technology, Gothenburg, Sweden, 2019. https://research.chalmers.se/publication/510102/file/510102_Fulltext.pdf.
- [12] J. Romani, G. Pérez, A. de Gracia, Experimental evaluation of a cooling radiant wall coupled to a ground heat exchanger, *Energy Build.* 129 (2016) 484–490, <https://doi.org/10.1016/j.enbuild.2016.08.028>.
- [13] J. Romani, L.F. Cabeza, P. Gabriel, A. Laura, A. De Gracia, Experimental testing of cooling internal loads with a radiant wall, *Renew. Energy* 116 (2018) 1–8, <https://doi.org/10.1016/j.renene.2017.09.051>.
- [14] A. Li, X. Xu, Y. Sun, A study on pipe-embedded wall integrated with ground source-coupled heat exchanger for enhanced building energy efficiency in diverse climate regions, *Energy Build.* 121 (2016) 139–151, <https://doi.org/10.1016/j.enbuild.2016.04.005>.
- [15] S. Javed, I.R. Ørnes, M. Myrup, T.H. Dokka, Design optimization of the borehole system for a plus-Energy kindergarten in Oslo, Norway, *Architect. Eng. Des. Manag.* (2018) 1–15, <https://doi.org/10.1080/17452007.2018.1555088>, 0.
- [16] D. Pahud, M. Belliard, P. Caputo, Geocooling potential of borehole heat exchangers' systems applied to low energy office buildings, *Renew. Energy* 45 (2012) 197–204, <https://doi.org/10.1016/j.renene.2012.03.008>.
- [17] J. Liu, X. Xie, F. Qin, S. Song, D. Lv, A case study of ground source direct cooling system integrated with water storage tank system, *Build. Simul.* 9 (2016) 659–668, <https://doi.org/10.1007/s12273-016-0297-0>.
- [18] T. Arghand, S. Javed, A. Trüschel, J. Dalenbäck, Control methods for a direct-ground cooling system : an experimental study on office cooling with ground-coupled ceiling cooling panels, *Energy Build.* 197 (2019) 47–56, <https://doi.org/10.1016/j.enbuild.2019.05.049>.
- [19] Z. Li, W. Zhu, T. Bai, M. Zheng, Experimental study of a ground sink direct cooling system in cold areas, *Energy Build.* 41 (2009) 1233–1237.
- [20] J. Kurmitski, nZEB office building Ympäristöälytalo in Helsinki, Finland, *REHVA Eur. HVAC J.* 44–49 (2012). <https://www.rehva.eu/rehva-journal/chapter/nzeb-office-building-ympaeristoetalo-in-helsinki-finland>.
- [21] J. Graslund, nZEB headquarters of Skanska, *REHVA Eur. HVAC J.* 44–47 (2014). <https://www.rehva.eu/rehva-journal/chapter/nzeb-headquarters-of-skanska>.
- [22] S.J. Rees, *Advances in Ground-Source Heat Pump Systems*, 2016.
- [23] M. Virta, D. Butler, J. Graslund, J. Hogeling, E.L. Kristiansen, *Chilled Beam Application Guidebook, Rehva Guidebook No 5*, 2005, ISBN 2-9600468-3-8.
- [24] M. Kottek, J. Grieser, C. Beck, B. Rudolf, F. Rubel, World map of the Köppen-Geiger climate classification updated, *Meteorol. Z.* 15 (2006) 259–263, <https://doi.org/10.1127/0941-2948/2006/0130>.
- [25] E.N. CEN, 15251- Indoor Environmental Input Parameters for Design and Assessment of Energy Performance of Buildings Addressing Indoor Air Quality, Thermal Environment, Lighting and Acoustics, European Committee for Standardization, Brussels, Belgium, 2007.
- [26] ISO, ISO 7730- Ergonomics of the Thermal Environment – Analytical Determination and Interpretation of Thermal Comfort Using Calculation of the PMV and PPD Indices and Local Thermal Comfort Criteria, International Organization for Standardization, Brussels, Belgium, 2014.
- [27] Swedish Work Environment Authority, Workplace design- Provisions of the Swedish Work Environment Authority on workplace design (AFS 2009:2), Arbetsmiljöverket, Stockholm, Sweden, 2009. <https://www.av.se/globalassets/filer/publikationer/foreskrifter/engelska/workplace-design-provisions-afs2009-2.pdf>.
- [28] ASHRAE, *ASHRAE Handbook - HVAC Fundamentals*, Am. Soc. Heating, Refrig. Air Cond. Eng. Atlanta, 2017.
- [29] K.P. Tsagarakis, L. Efthymiou, A. Michopoulos, A. Mavragani, A.S. Andelković, F. Antolini, M. Bacic, D. Bajare, M. Baralis, W. Bogusz, S. Burlon, J. Figueira, M.S. Genç, S. Javed, A. Jurelionis, K. Koca, G. Rzyński, J.F. Urchueguia, B. Zlender, A review of the legal framework in shallow geothermal energy in selected European countries: need for guidelines, *Renew. Energy* 147 (s) (2020) 2556–2571, <https://doi.org/10.1016/j.renene.2018.10.007>.
- [30] S. Javed, Design of Ground Source Heat Pump Systems: Thermal Modelling and Evaluation of Boreholes, Chalmers University of Technology, Gothenburg, Sweden, 2010.
- [31] J.D. Spitler, S. Javed, R.K. Ramstad, Natural convection in groundwater-filled boreholes used as ground heat exchangers, *Appl. Energy* 164 (2016) 352–365, <https://doi.org/10.1016/j.apenergy.2015.11.041>.
- [32] S. Javed, J.D. Spitler, P. Fahlén, An experimental investigation of the accuracy of thermal response tests used to measure ground thermal properties, *ASHRAE Trans.* 117 (2011) 13–22.
- [33] T. Arghand, A. Trüschel, J.-O. Dalenbäck, S. Javed, Dynamic thermal performance and controllability of dry fan-coil unit, in: *Cold Clim. HVAC Conf.*, Springer, 2018, pp. 351–361, <https://doi.org/10.1007/978-3-030-00662-4>.
- [34] S. Moosberger, Report: IDA ICE CIBSE-Validation: test of IDA Indoor Climate and Energy version 4.0 according to CIBSE TM33, issue 3, Lucerne University of Applied Sciences and Arts, Luzern, Switzerland, 2007. http://www.equonline.com/iceuser/validation/ICE-Validation-CIBSE_TM33.pdf.
- [35] EQUA Simulation Technology Group, Technical report: Validation of IDA Indoor Climate and Energy 4.0 build 4 with respect to ANSI/ASHRAE Standard 140-2004, EQUA Simulation Technology Group, Stockholm, Sweden, 2010.
- [36] S. Kropf, G. Zweifel, Validation of the building simulation program IDA-ICE according to CEN 13791 “thermal performance of buildings - calculation of internal temperatures of a room in summer without mechanical cooling - general criteria and validation procedures”, Lucerne University of Applied Sciences and Arts, Luzern, Switzerland, 2001.
- [37] A.B. Equa Simulation, User guide: borehole 1.0. <http://www.equonline.com/iceuser/pdf/UserGuideBoreholes.pdf>, 2014.
- [38] L. Eriksson, P. Skogqvist, Description of the IDA ICE borehole model, *Internal Report, EQUA Simulation Technology Group, Stockholm, Sweden*, 2017.
- [39] L. Liu, Z. Yu, H. Zhang, H. Yang, Performance improvements of a ground sink direct cooling system under intermittent operations, *Energy Build.* 116 (2016) 403–410, <https://doi.org/10.1016/j.enbuild.2016.01.032>.
- [40] X. Cao, Y. Yuan, L. Sun, B. Lei, N. Yu, X. Yang, Restoration performance of vertical ground heat exchanger with various intermittent ratios, *Geothermics* 54 (2015) 115–121, <https://doi.org/10.1016/j.geothermics.2014.12.005>.
- [41] J.R. Cullin, J.D. Spitler, C. Montagud, F. Ruiz-Calvo, S.J. Rees, S.S. Naicker, P. Konečný, L.E. Southard, Validation of vertical ground heat exchanger design methodologies, *Sci. Technol. Built Environ.* 21 (2015) 137–149, <https://doi.org/10.1080/10789669.2014.974478>.
- [42] J.R. Cullin, J.D. Spitler, A computationally efficient hybrid time step methodology for simulation of ground heat exchangers, *Geothermics* 40 (2011) 144–156, <https://doi.org/10.1016/j.geothermics.2011.01.001>.
- [43] R. Kosonen, J. Penttinen, The effect of free cooling and demand-based ventilation on energy consumption of self-regulating and traditional chilled beam systems in cold climate, *Indoor Built Environ.* 26 (2017) 256–271, <https://doi.org/10.1177/1420326X16683236>.
- [44] P. Filipsson, A. Trüschel, J. Gräslund, J. Dalenbäck, Performance evaluation of a direct ground-coupled self-regulating active chilled beam system, *Energy Build.* 209 (2020), <https://doi.org/10.1016/j.enbuild.2019.109691>.
- [45] P. Eskilson, Thermal Analysis of Heat Extraction Boreholes, Department of Mathematical Physics, University of Lund, Sweden, 1987.